

Ab-initio density functional studies of stepped TaC surfaces

V. B. Shenoy and C. V. Ciobanu

Division of Engineering, Brown University, Providence, RI 02912

(Dated: November 10, 2018)

We report on density functional total energy calculations of the step formation and interaction energies for vicinal TaC(001) surfaces. Our calculations show that double and triple-height steps are favored over single-height steps for a given vicinal orientation, which is in agreement with recent experimental observations. We provide a description of steps in terms of atomic displacements and charge localization and predict an experimentally observable ruffled structure of the step-edges, where the Ta atoms undergo larger displacements compared to the C atoms.

The stepped surfaces of transition metal carbides (TiC, TaC, etc.) are technologically important due to their applications as surface catalysts with high corrosion resistance. From a fundamental point of view, these surfaces have received attention as they provide a rich ground for studying faceting transitions that involve single and multiple-height steps. In a series of experiments, Zuo and coworkers [1]–[4] have investigated the structure of several surfaces vicinal to TaC(001) and found that multiple-height steps are favored over single-height steps in all the cases. Motivated by these experiments, we perform ab-initio density functional calculations to obtain the first quantitative results for the step formation and interaction energies for steps of different heights on these surfaces.

The preference for single or multiple-height steps for a certain vicinal orientation is determined by the energy required to create an isolated step of a certain height and the repulsive interactions between these steps. In general, it costs more energy to create multiple-height steps, as the number of bonds that are broken in the process of creating a step increases with its height. On the other hand, the energetic contribution from the repulsive step-step interactions can be the lower in the case of a vicinal surface with multiple-height steps due to a lowering of the number of step pairs per unit length. As we will see, both of these effects are borne out by our calculations. Furthermore, we will show that the increase in the formation energies of double and triple-height steps over the single-height steps is not large enough to offset the effect of step-step interactions. Consequently, the former types of steps are favored for the vicinal orientations that we consider. In what follows, we also will report on the structures of different types of steps in terms of charge density and atomic displacements, and develop a phenomenological model for the electrostatic step interactions.

The density functional calculations were carried out with the VASP package [5], using the projector augmented-wave pseudopotentials [6] and the Perdew-Wang functional form [7] for exchange correlation energy. Bulk calculations with an 8-atom cell and a 35 k-point Brillouin zone sampling gave an optimum Ta-C separation of $a = 2.2415\text{\AA}$. For surface calculations, the

	d_C^1	d_{Ta}^1	d_C^2	d_{Ta}^2	r_1	r_2
Exp. [8]	0.09	-0.11	0.04	0.00	0.20	0.04
Theor. [10]	0.097	-0.132	–	–	0.23	0.052
This work	0.077	-0.115	0.027	-0.008	0.192	0.035

TABLE I: Ruffling relaxation of TaC(001) compared with previous results [8], [10]. The displacements of the first ($d_{C,Ta}^1$) and second ($d_{C,Ta}^2$) layer surface atoms, and the ruffling amplitudes r_1 , r_2 (defined in [8]) are given in \AA .

Brillouin zone was sampled using a Γ -centered $8 \times 8 \times 1$ grid. This sampling yielded 15 k-points for TaC(001) and 21 to 25 k-points for the vicinal surfaces. The ions were relaxed using a conjugate-gradient algorithm until the total energy converged to 0.01eV. The energy cut-off for the plane waves was set to 400eV (29.40 Ry) in all the calculations.

Before we proceed with the discussion of vicinal surfaces, we compare the predictions of the surface structure of TaC(001) obtained using the present model with experimental observations and previous theoretical studies. It is well-known [8]–[10] that this surface exhibits a ruffling reconstruction, where the C atoms are displaced out of the surface while the Ta atoms are pulled inwards. It can be seen from Table I that our results for the relative displacements of the atoms in the first and second surface layers are in close agreement with available experimental [8] and theoretical [10] data.

For vicinal surfaces, we used supercells as illustrated in Fig. 1, where L_x and L_z denote the terrace-width of the stepped surface and height of the supercell, respectively. The dimension of the supercell in the y -direction (L_y) is determined by the period in the direction parallel to the step, which in the present case is the lattice constant of TaC, $2a$. To create the steps, we employ shifted (i.e. non-orthogonal) boundary conditions [11], in which the amount of shift in the z -direction determines the height of the steps. The structures of the single (Sh), double (Dh) and triple (Th) -height steps that we consider in the present work are shown in Fig. 1. All calculations on vicinal surfaces were carried out using a slab of TaC with 8 atomic rows (17.932\AA) and a vacuum thickness of 10\AA . In order to ensure that these results are not influenced by

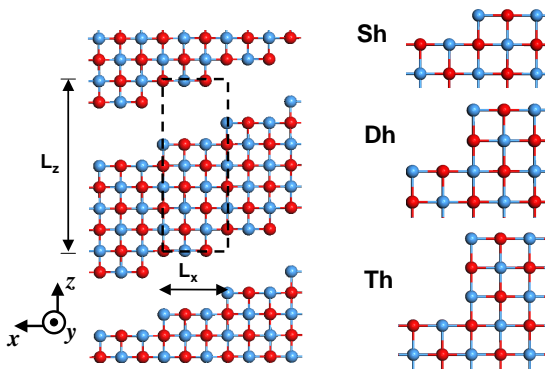


FIG. 1: Geometry of a typical stepped surface, with the supercell indicated by dashed lines. The structures of the single (Sh), double (Dh) and triple (Th) -height steps considered in the present work are also given in the figure.

n	λ_n^f (meV/Å)	λ_n^d (meVÅ)	β_n^f (meV/Å ²)	β_n^d (meV/Å ²)
1	268.89	998.42	119.96	88.85
2	466.47	550.34	104.05	6.11
3	637.08	1217.92	94.74	4.01

TABLE II: Step formation energies λ_n^f and repulsion strengths λ_n^d obtained using linear fits of data in Fig. 2 to Eq. (1). The table also shows the scaled step formation energies β_n^f and interaction strengths β_n^d introduced in Eq. (2).

finite-size effects, we repeated the calculations for certain selected step structures and terrace widths by increasing the cell thickness to 10 atomic rows and the dimension of the vacuum to 15Å; the results were found to change by less than 5% in all the cases that were considered.

The energetics of stepped surfaces can be understood by considering the ledge energy, defined as $\lambda_n = (E - N_p e_b - \gamma_0 A) / 2L_y$ [11], where E is the total energy of the N_p Ta-C pairs in the slab, $e_b = -22.1536$ eV is the bulk energy per pair, $\gamma_0 = 95.53$ meV/Å² is the surface energy of the TaC(001) surface and the subscript n denotes the step-height. The ledge energy is the energy per unit length of the vicinal surface in excess of the surface energy of the terraces that separate the steps, and includes both the step formation and interaction energies. Using the fact that both the elastic and electrostatic effects give rise to dipolar interactions [12, 13], the ledge energy can be expressed as

$$\lambda_n = \lambda_n^f + \frac{\lambda_n^d}{L_x^2}, \quad (1)$$

where λ_n^f and λ_n^d denote the formation energy and the dipolar interaction strength of a step with height na , respectively. The computed ledge energies for the three types of steps are plotted in Fig. 2, along with linear

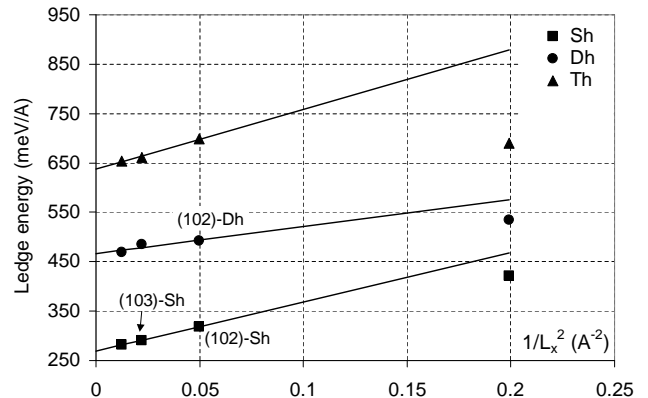


FIG. 2: Ledge energies λ for the single (Sh), double (Dh) and triple (Th) height steps plotted as a function of $1/L_x^2$. The points for which the step separations exceed $a = 2.24$ Å are fit to Eqn. (1), $\lambda_n = \lambda_n^f + \lambda_n^d / L_x^2$ [14]. Parameters λ_n^f , λ_n^d are given in Table II.

(hkl)	step	γ (from data in Fig. 2)	γ (from Eq. (2))
(102)	Sh	149.01	146.71
	Dh	132.22	131.67
	Th	–	127.46
(103)	Sh	131.66	131.66
	Dh	–	123.74
	Th	–	120.73

TABLE III: Surface energies (in meV/Å²) of the (102) and (103) surfaces considered by Zuo and coworkers in [3]. The table gives surface energies calculated using Eq. (2) and the scaled fitting parameters in Table I, as well as surface energies for (102)-Sh and Dh and (103)-Sh calculated directly from the ledge energies marked in Fig. 2. The close agreement between the surface energies obtained using the two different approaches indicates that Eq. (1) gives an accurate description of the ledge energies.

fits to the functional form assumed in Eq. (1) [14]. The fitting parameters λ_n^f and λ_n^d are given in Table II.

It can be seen from Table II that the formation energies of the steps increase with their heights, in agreement with bond counting arguments presented earlier. The dipolar interactions, on the other hand, do not show a monotonic trend; the interaction strength of the Dh step is smaller than the corresponding values for the Sh and Th steps. The relative importance of these two contributions can be understood by considering the surface energy of a vicinal surface made of steps with height na , given by

$$\gamma_n(\theta) = \gamma_0 \cos \theta + \beta_n^f |\sin \theta| + \beta_n^d \frac{|\sin^3 \theta|}{\cos^2 \theta}, \quad (2)$$

where θ is the vicinal angle and the parameters $\beta_n^f = \lambda_n^f / (na)$ and $\beta_n^d = \lambda_n^d / (na)^3$ denote scaled step formation and interaction contributions, respectively. Using

the values of these parameters tabulated in Table II, we find that both the scaled formation and interaction parts show a monotonic decrease with increasing step height, indicating that multiple-step heights are favored over the single height steps for any vicinal orientation. In the following paragraph we consider experimental work of Zuo and coworkers [1]–[4] and show that the predictions of our calculations are in agreement with their observations.

Using a statistical analysis [15] of the step separation distributions on TaC(103) and (102) surfaces, Zuo and coworkers have determined that the former surface consists of a large number of triple-height steps and a smaller number of double-height steps while the latter surface consists of almost equal amounts of areas that contain either triple or quadruple-height steps. In order to understand these results, in Table III, we have used Eq. (2) and the data in Table II to calculate the surface energies of these vicinal surfaces made up of Sh, Dh and Th steps. For both the surfaces considered in the experimental work, we find that the single-step vicinal is much larger (by $\sim 10\text{-}20 \text{ meV}/\text{\AA}^2$) in energy than the vicinals with multiple-height steps. Furthermore, the triple-height steps are favored over the double-height steps (by $\sim 4 \text{ meV}/\text{\AA}^2$) in both the cases, explaining their stability and their presence on (103) and (102) surfaces. The presence of a few Dh steps and the complete absence of Sh steps on (103) surfaces is consistent with the fact that the former is closer in energy to the Th steps than the latter by about $8 \text{ meV}/\text{\AA}^2$ (refer to Table III). At the present time, we are unable to consider the energetics of quadruple-height steps due to the size of this model [16].

We now turn our attention to the description of the steps in terms of the atomic displacements at the step-edges, which are shown in Fig. 3 for the (105)-Sh and the (102)-Dh surfaces. The figure shows that the atoms at the step-edges undergo both horizontal (x) and vertical (z) displacements. On moving a few atomic spacings away from the step-edge, the atoms on the terraces are predominantly displaced in the vertical direction, as in the case of the (001) surface. Overall, the displacement field of the step resembles the field produced by a force-dipole [12] located at the step-edge, though there are new features that emerge. In particular, the step-edge is rumpled, such that the horizontal displacements of the Ta atoms at the step-edges are significantly larger than the corresponding displacements of the C atoms. Since both the components of the rumpling vector \mathbf{s} given in Fig. 3 are comparable to the rumpling amplitudes for Ta(001) given in Table I, we believe that this effect could be observed in experiments. The step rumpling also leads to formation of electric dipoles, which will be considered next.

The magnitudes of the electric dipoles at the step-edges due to rumpling can be estimated as $Q|\mathbf{s}|$, where Q is the amount of charge transferred from C to Ta due to the partially ionic character of the TaC-bond. Since $Q \sim |e|$

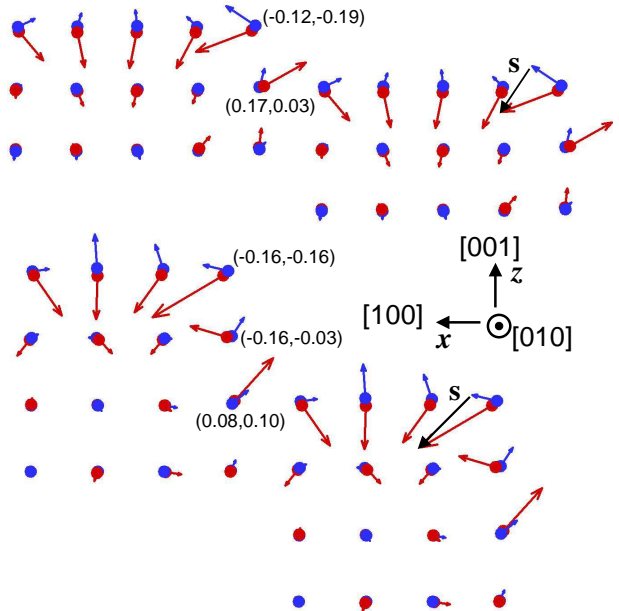


FIG. 3: Atomic displacements of the TaC(105) and TaC(102) surfaces with Sh steps (top) and Dh steps (bottom), respectively. All vectors lie in the xz plane and have been magnified for clarity. Each atomic row is characterized by a rumpling vector, whose components are given by the difference in displacements of the Ta (red) and C (blue) atoms. The rumpling vector \mathbf{s} of the atomic row at the step-edge is marked in the figure. The components of the rumpling vectors (in \AA) for a few atomic rows near the step-edge are also given in the figure.

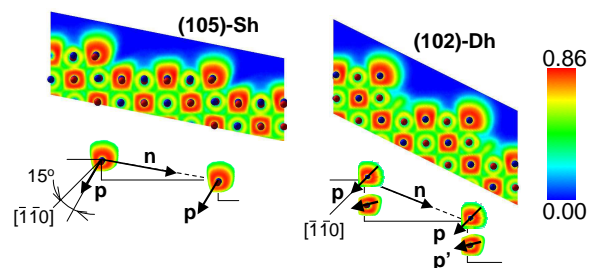


FIG. 4: Electron localization function (arbitrary units) in the (010) cross-section for TaC(105)-Sh and TaC(102)-Dh surfaces. The dipoles of the C atoms at the step-edges are denoted by \mathbf{p} . In the case of the Dh step, \mathbf{p}' denotes the dipole of the C atom located below the Ta atom at the step-edge in the plane immediately behind the one shown in the figure.

and $|\mathbf{s}| \sim 0.1a$ (refer to Fig. 3), where e is the electronic charge, the linear dipole density due to step rumpling is $P \sim 0.1|e|$. In addition to the dipoles that arise as a result of step-rumpling, we also find that there are additional dipoles that are created due to charge distortions at the step-edge. We observe that the valence shell

around the C atoms expands out of the surface leading to formation of electric dipoles, denoted by \mathbf{p} and \mathbf{p}' in Fig. 4. Such electronic distortions also exist for the Ta surface atoms, but to a much smaller extent. The magnitude of these dipoles can be obtained from the electron localization functions, which are shown in Fig. 4 for the (105)-Sh and the (102)-Dh surfaces. Our calculations show that the typical magnitude the linear dipole density due to charge spill-out at the step-edge is $P \sim 0.3-0.7|e|$.

The interaction energy between steps characterized by the effective electrostatic dipole density \mathbf{P} and the force moment $\mathbf{D} = (D_x, D_z)$ is given by [12, 13] :

$$\frac{\lambda_n^d}{L_x^2} = \frac{\pi^2(P_\perp^2 - P_\parallel^2)}{3L_x^2} + \frac{\pi(1 - \nu^2)(\tau^2 n^2 a^2 + D_x^2)}{3EL_x^2}, \quad (3)$$

where P_\parallel (P_\perp) is the component of \mathbf{P} parallel (perpendicular) to the unit-vector \mathbf{n} in Fig. 4, τ is the surface stress which generates the z -component of the elastic dipole moment ($D_z = \tau n a$), E is the Young's modulus, and ν is the Poisson's ratio [17]. While separating the elastic and electrostatic contributions to step interactions is a difficult task, we can use the information from Fig. 4 to obtain estimates for these two effects.

First, observe that the dipole density due to step-rumpling is about 20-30% of the dipole density arising from charge spill-out; it is therefore reasonable to calculate the electrostatic interactions by focusing on the latter effect. Next, we see from Fig. 4 that compared to the Sh-step, the Dh-step has a larger value of P_\parallel due to the presence of an additional C atom with dipole \mathbf{p}' that is aligned closely with the vector \mathbf{n} . With increasing step-height, the number of such atoms increases, leading to even larger values of P_\parallel and a monotonic *decrease* in the electrostatic contribution (refer to Eq. (3)). However, we see from Table. II that the step interaction parameters show a non-monotonic trend, which we attribute to an increase in the strength of elastic interactions with the height of steps in the following paragraph.

Using Eq.(3), we calculate the electrostatic contribution to the interactions of Sh steps to be $\approx 1\text{eV}\text{\AA}$, which is close to the value of λ_1^d given in Table II, indicating that the step interactions are dominated by the electrostatic effects. This observation is also in agreement with the fact that a typical value of surface stress $\tau \approx 100\text{meV}/\text{\AA}^2$ yields a small repulsive elastic contribution which is $\approx 0.01\text{meV}\text{\AA}$. In the case of Dh-steps, a decrease in step interaction parameter (λ_2^d) is consistent with a decrease in the electrostatic contribution with increasing step-height. However, a subsequent increase in the interaction parameter (λ_3^d) for the Th-step can only be explained if the magnitude of the elastic dipole, $|D| = \sqrt{D_x^2 + D_z^2}$ increases with the height of the step. In this case, we expect both the electrostatic and elastic contributions to be comparable in magnitude.

In summary, by calculating step formation and interaction energies we have shown that Dh and Th steps lead

to more stable vicinal surfaces, a result consistent with experimental observations [1]–[4]. We have described the atomic displacements of the surfaces and proposed a simple model for the electrostatic interaction of the steps in terms of electric dipoles of carbon atoms and step rumpling.

We gratefully acknowledge research support from the National Science Foundation through grants CMS-0093714 and CMS-0210095 and the Brown University MRSEC program. Computational support for this work was provided by the National Center for Supercomputing Applications through grant DMR-020032N and the Graduate School at Brown University through the Salomon Research Award.

-
- [1] J. K. Zuo and D. M. Zehner, Phys. Rev. B **46** 16122 (1992).
 - [2] J. K. Zuo, R. J. Warmack, D. M. Zehner and J. F. Wendelken, Phys. Rev. B **47**, 10743 (1993).
 - [3] J. K. Zuo, J. M. Carpinelli, D. M. Zehner and J. F. Wendelken, Phys. Rev. B **53**, 16013 (1996).
 - [4] J. K. Zuo, T. Zhang, J. F. Wendelken and D. M. Zehner, Phys. Rev. B **63**, 33404 (2001).
 - [5] G. Kresse and J. Furthmuller, Phys. Rev. B **54**, 11169 (1996) and Comput. Mater. Sci. **6**, 15 (1996).
 - [6] G. Kresse, and J. Joubert, Phys. Rev. B **59**, 1758 (1999).
 - [7] J. Perdew and Y. Wang, Phys. Rev. B **45**, 13244 (1992).
 - [8] G. R. Gruzalski, D. M. Zehner, J. R. Noonan, H. L. Davis, R. A. Dio and K. Müller, J. Vac. Sci. Technol. A **7**, 3 (1989) and references therein.
 - [9] D. L. Price, J. M. Willis and B. R. Cooper, Phys. Rev. Lett. **77** 3375 (1996) and Phys. Rev. B **48**, 15301 (1993).
 - [10] K. Kobayashi, Jpn. J. Appl. Phys. **39**, 4311 (2000); K. Kobayashi, Surf. Sci. **493**, 665 (2001).
 - [11] T. W. Poon, S. Yip, P. S. Ho and F. F. Abraham, Phys. Rev. B **46**, 16122 (1992).
 - [12] V. I. Marchenko and Y. A. Parshin Sov. Phys. JETP **52**, 129 (1980).
 - [13] C. Jayaprakash, C. Rottmann, and W. F. Saam, Phys. Rev. B **30**, 6549 (1984); A. Redfield and A. Zangwill Phys. Rev. B **46**, 4289 (1992).
 - [14] The fact that the point corresponding to $L_x = 2.24\text{\AA}$ lies *below* the linear fit (Fig. 2) indicates the presence a short-range attraction between the steps, which has also been inferred from experimental observations in Ref. [4]. We defer a discussion on the origin of this short-range interaction to a later publication.
 - [15] B. Joós, T. L. Einstein and N. C. Bartelt, Phys. Rev. B **43**, 8153 (1991).
 - [16] Calculations of the energetics of quadrupole-height steps become very demanding because, in addition to increased terrace width, this system also requires larger slab and vacuum thickness (more plane waves) in order to ensure that the interactions involving the slab-faces and the slab-corners are small.
 - [17] The elastic constants for TaC are taken from L. E. Toth, *Transition Metal Carbides and Nitrides* (Academic Press, New York, 1971), page 148.